Derivation of MSL Riverbank Line from UAV DSM Data based on Tidal Slope Analysis

Preprint · December 2020

CITATIONS
0

READS
44

3 authors, including:

Norhafizi Mohamad
Universiti Teknologi Malaysia
26 PUBLICATIONS **35** CITATIONS
SEE PROFILE

Ami Hassan Md Din
Universiti Teknologi Malaysia
103 PUBLICATIONS **412** CITATIONS
SEE PROFILE

Derivation of MSL Riverbank Line from UAV DSM Data based on Tidal Slope Analysis

Derivation of MSL Riverbank Line from UAV DSM Data based on Tidal Slope Analysis

N Mohamad[1*], A Ahmad[1,2*], and A H M Din[1,2]

[1]Department of Geoinformation, Faculty of Built Environment and Surveying, Universiti Teknologi Malaysia (UTM), Johor Bahru 81310, Malaysia
[2]Geomatics Innovation Research Group (GnG), Faculty of Built Environment and Surveying, Universiti Teknologi Malaysia (UTM), Johor Bahru 81310, Malaysia

pijieypih@gmail.com, anuarahmad@utm.my

Abstract. Deriving a riverbank line at a tidal river is complicated, since dynamic factors such as tide and slope topography influence its location. Hence, this study utilises the Unmanned Aerial Vehicle (UAV), geodetic, and tidal data to identify the exact riverbank line based on Mean Sea Level (MSL) value from UAV products. We carried out two epochs of UAV data collection during low and high tide conditions. Orthometric height (H) has been applied in UAV data processing to produce a high accuracy of orthophoto and Digital Surface Model (DSM). UAV-MSL derived riverbank lines have been identified from the UAV orthophoto image using supervised classification and feature extraction techniques. DSM model provides the topographical height in three-dimensional (3D) view and enables identifying low and high tide, MSL, and lowest astronomical tides (LAT) at the riverbank. The study found that UAV-MSL derived riverbank line was identified in between the MSL value (at 2.302 m) and chart datum (at 1.043 m). This study also identified the correlation model, R^2 value at 0.9288 between UAV-MSL derived riverbank line with MSL-tide gauge data. This study provides an alternative for researchers to determine riverbank lines based on UAV derived MSL instead of using only tide gauge data.

1. Introduction

Riverbank line is a land-water boundary that shows how far the water can reach the land, and some boundaries, such as dry-wet, in the coastal region, will leave a mark [1, 2]. However, the riverbank line is dynamic and always varied on few factors, such as rising sea levels, tidal effects, erosion and sedimentation, that affect the riverbank line position [3]. The riverbank line has been delineated by wet and dry line mark in any orthophoto or satellite image without considering tide and slope elements [4]. All geodetic elements including ellipsoid, geoid, and orthometric height are incorporated to identify the real riverbank line at the tidal river, [9]. Although riverbank line is not entirely affected by tide, however, the tide factor still dominant in surface water level dynamics if no significant weather changes (i.e; storm surges, cyclone, etc.) exists during study period. Sea level rise (SLR) also affects the surface water level, but with a tiny change ranged at 0.054 m from year 1993 to 2015, while absolute sea level rate is 3.27 ± 0.12 mm yr-1 at Malacca Strait's region [5]. The riverbank lines are determined based on tidal datum measurement since the number of water level transition from low to high and high to low are significantly high, ranges 0.5 to 4 m [6, 7]. However, the amount of tidal correction is depending on the tidal range and slope height characteristics [8].

This study attempts to utilises Unmanned Aerial Vehicle (UAV), geodetic, and tidal data to identify the exact riverbank line based on Mean Sea Level (MSL) value. We collected UAV data to produce the orthomosaic at different tide levels and DSM, thus showing the riverbank slope changes during low and high tide. For GNSS measurement, we have used the northing and easting coordinates by referring to orthometric height (H). Horizontal and vertical data from the GNSS survey are necessary for Ground Control Point (GCP) establishment and for calculating the orthometric height. The resulting orthometric height in the 3D profile view was projected into two-dimensional (2D) views for mapping and data verification purposes. The final output incorporated the UAV-MSL riverbank line and has been verified with MSL data from the tide gauge.

2. Materials and Method

2.1. Study Area

The location of study area, Kilim River, Langkawi, Kedah (Figure 1) is at the 6°21.518'- 6°26.093' N and 99°51.159 - 99°51.159' E at northern part of Malacca Straits. The study area has been recognised as a part of UNESCO Kilim Kast Geoforest Park (KKGP) in 2007. The Kilim River experienced two high and two low tides per day (semi-diurnal types) [9-11]. Although Kilim River is approximately three kilometres from the coastal zone, the tidal effect still exists and affects the Kilim River hydrodynamically. During the tidal phenomenon, the water level increased approximately 12 hours and 25 minutes apart, and it takes 6 hours, 12 minutes, and 30 seconds to move from low to high tide and vice versa.

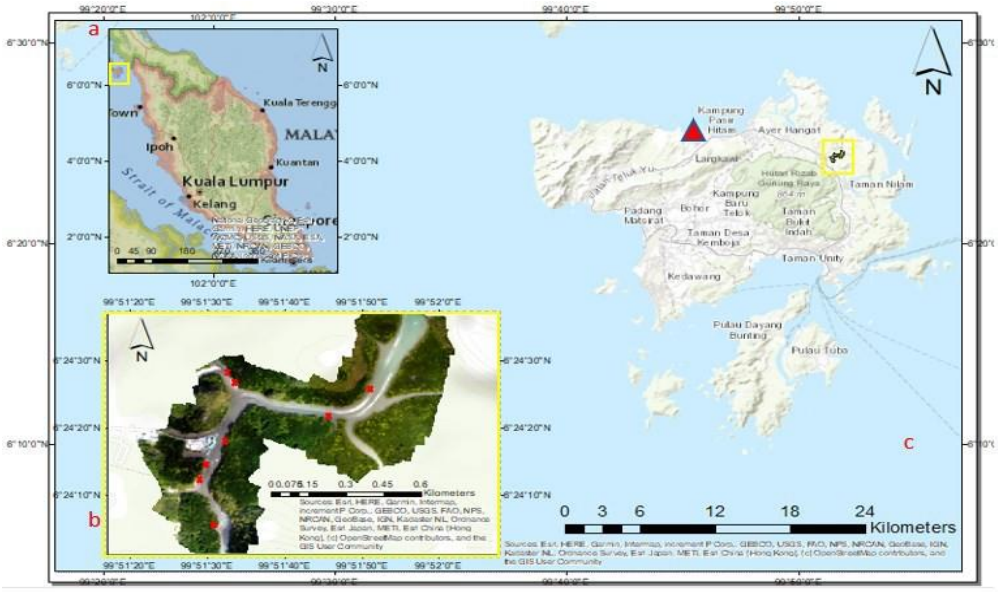

Figure 1. (a) Location of the study area in Peninsular Malaysia (showed by small yellow square); (b) Location of Kilim River as the primary study area displayed in the orthomosaics image captured from UAV (The red 'X' marks represent the GCP point to georeferencing the image; (c) Location of the specific study area in the map of Langkawi Island, Kedah (showed by small yellow square) and Department of Survey and Mapping Malaysia (DSMM) tide gauge (TG3) at Langkawi.

2.2. Data

2.2.1. GNSS Data. We conducted GNSS measurements in December 2017 using Topcon GR-5 model. During measurement, we established eight stations at the study area, and all stations are well-distributed. We used the static technique for one-hour observation at each GCP stations, and each of the measurements refers to the Continuously Operating Reference Station (CORS) at Langkawi and

Arau.

According to Table 1, we measured all stations to get the latitude, longitude, and height of the earth surface, which later used as Ground Control Point (GCP) for UAV data processing (Figure 1b). We used Geocentric Datum of Malaysia 2000 (GDM 2000) which also known as the local state coordinate system for Kedah and Perlis region. The orthometric height has been identified by subtracting the ellipsoid height (GNSS survey) with the geoid height (MyGeoid model) to ensure the vertical data (orthometric height) reached the global mean sea level (MSL). Hence, the insert vertical datum during image processing was based on orthometric height as shown in Table 1. Based on Equation (1), geoid height, we required N along with ellipsoid height (h) to form orthometric height, H, which later could determine the exact height of earth topography.

$$H = h - N \quad (1)$$

Table 1. GNSS measurement using static method for GCP data acquisition.

Station	Latitude (N)	Longitude (E)	Ellipsoid height (m)	Geoid height (m)	Orthometric Height (m)
1	6°24'14.92913"	99°51'29.89778"	-13.542	-15.476	1.934
2	6°24'13.22827"	99°51'29.31088"	-13.506	-15.476	1.970
3	6°24'06.44999"	99°51'30.99053"	-12.892	-15.470	2.578
4	6°24'18.56162"	99°51'32.29534"	-13.395	-15.476	2.081
5	6°24'26.35379"	99°51'33.75353"	-13.495	-15.479	1.984
6	6°24'27.89381"	99°51'32.83221"	-13.693	-15.481	1.788
7	6°24'21.38469"	99°51'45.54535"	-13.451	-15.464	2.013
8	6°24'24.46398"	99°51'50.43701"	-13.344	-15.460	2.116

2.2.2. UAV Photogrammetry Data. We collected two epochs of UAV data at Kilim River in December 2017. We carried UAV data collection out during low and high tide conditions using the DJI Phantom 4 Advanced model, which operated based on the multi-rotor system. Two flights required to cover the study area for each epoch. Epoch 1 (20 December 2017) has been collected during high tide, while epoch 2 (20 December 2017) has been collected during low tide. The average flying height for epoch 1 is 184 m while epoch 2 is 228 m above ground level, which generated images with a 4.7 cm spatial resolution at epoch 1 and 5.6 cm at epoch 2. The flight plan has been created using DJI GO software. 116 images were captured at epoch 1 and 252 images were captured at epoch 2 to cover entire study area.

2.2.3. Tidal Data. One month of tidal data of December 2017 acquired from one of the well-established tide gauges at Langkawi Island (Figure 1a). As mentioned in the earlier sub-section 2.1, the study area has two high tides and two low tides per day. Tidal data are auto-recorded in a one-hour interval, including tide reading in two high tides and two low tides. We computed MSL by averaging the total daily reading as a mean value, while LAT value has identified based on smallest reading in the monthly data. Tidal data from Department of Survey and Mapping Malaysia (DSMM) was already calculating the value of MSL and LAT for tidal analysis. These data are essential for validating the accuracy of water level between UAV and tide gauge-based measurement [9].

2.3. Methods

2.3.1. Generation of Orthophoto and DSM from UAV. This study required two orthomosaic images covering the Kilim River's condition during low and high tides. During high tide, UAV captured 126 shots at the 130-meter altitude above MSL, while at low tide, UAV captured 116 images at 130-meter height. Generating orthomosaic and DSM using Agisoft Metashape software started by aligning all digital aerial images, followed by building mesh. Later, the GCP marker coordinates have been inserted

manually from GNSS data in section 2.2.1, and for the altitude, the orthometric height was used to calculate accurate vertical data, H. It optimised camera alignment to achieve a higher accuracy of camera external and internal orientation parameters and correcting the distortion. Then, the aligned aerial digital aerial images have been converted into a dense point cloud using dense cloud build command in Agisoft software. Afterward, the dense point cloud has been generated using the build mesh command and followed by building the texture. The last step in Agisoft Metashape software workflows is to generate DSM and orthomosaic model.

2.3.2. Identification of Riverbank Line using Image Classification Technique. The image classification process started by creating the feature class such as the river, hill, mangrove forest, jetty, and open area classes. Six training samples have been established at each feature class as the land cover type of interest and followed by image classification using Maximum Likelihood Classification (MLC). We formed the classified image of the Kilim River after the classification process. It comprised land cover elements based on the feature class and training sample data. The next process was to exporting the raster data format of a classified image into a polygon data type which purposely to identifying and extracting the riverbank line features from polygon data types using the feature selection tool.

Later, the river feature has been extracted from orthomosaic images and transformed into line types representing the riverbank conditions during high and low tides. Then, the extracted riverbank line features were overlaid with each other to observe the 2D difference of position between low and high tide riverbank line. Using Global Mapper software, the river profile was reprojected as 2D line based on orthometric height. Hence, this study focused on four sections (A-D), such as highlighted in Figure 2. In every section, we set the river transect lines across the end-to-end riverbank to display the profile of the surface water levels. The river transect lines formed a 20-meter intervals, where the number of cross-section lines is depend on the selected region's location.

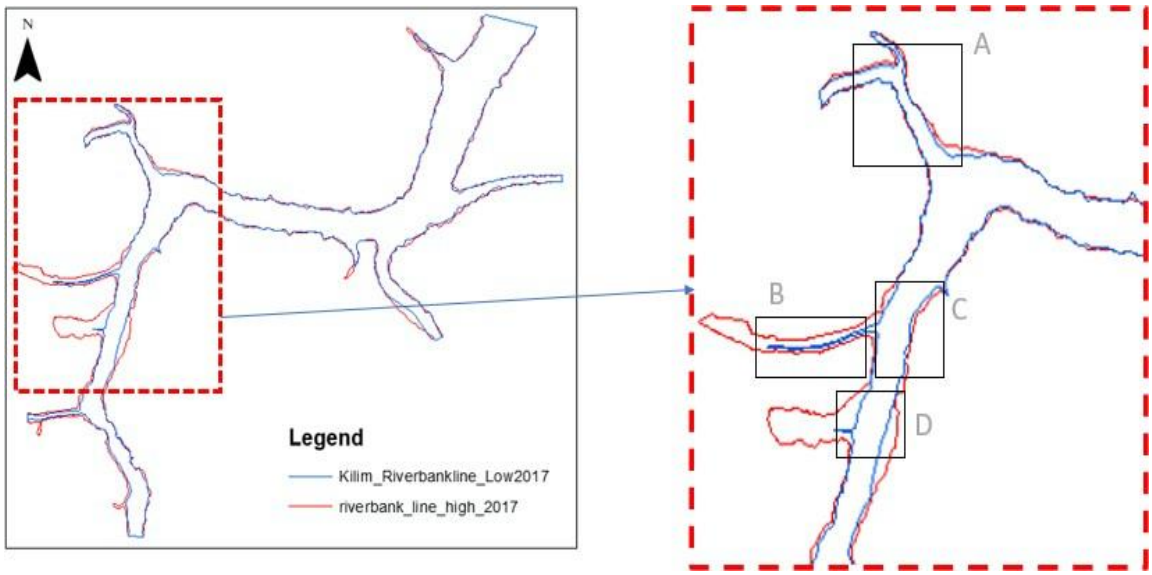

Figure 2. The overlaid riverbank line at Kilim River during low and high tides focused on the area marked with alphabets A until D. The reason is that this area is not covered by mangrove canopy, which makes it known as bare earth topography.

2.3.3. Identification of UAV-MSL Derived Riverbank Line. The classified and extracted riverbank lines from UAV images were still insufficient and created uncertainty within the dynamic river issue. Hence, the key to overcome the uncertainty is by determining the Mean Sea Level (MSL) value and estimating the exact riverbank line location based on MHW and MLW levels. We referred MLW and

MHW to riverbank line locations from UAV classified images during high and low tides, where both tide levels have been converted into 3D views in Figure 3. The DSM model provided the 3D view of the riverbank and the slope profile using Global Mapper software.

MHW and MLW's location created a triangle comprising tides and slope at the riverbank. The triangle in Figure 3 estimated the average tide level by calculating the slope value. Equation (2) explained the basis for finding the slope's value by utilising an elevation triangle of elevation for X and Y coordinates. After we have identified slope value, we computed the MSL value to find the mean 3D slope distance at the riverbank. Then, the tidal range was needed to estimate water height between MHW and MLW by calculating the mean value of 3D slope distance, as represented in Equation (2).

$$Riverbank\ Slope, M = \frac{\Delta Y}{\Delta X} \tag{2}$$

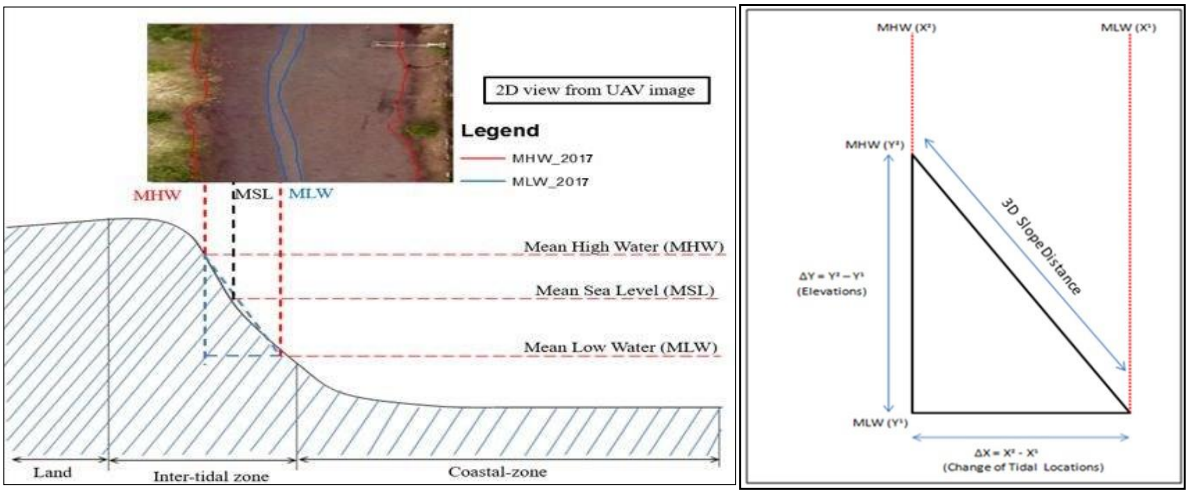

Figure 3. The 3D view from UAV image which shows the position of MHW, MSL and MLW at the riverbank slope (Left); The triangulated view of each tide condition (Right).

3. Results and Discussion

3.1. Determine the Position of UAV Derived MSL Riverbank Line in 3D Reprojected View

We measured MSL and LAT value at 2.302 m and 1.043 m by averaging one-month tidal data. LAT has been derived based on the smallest reading of tidal data in December 2017, and we have considered this value as the lowest astronomical tide level at the month based on December 2017 tide reading data. We projected both MSL and LAT values into 3D riverbank view. The coordinates of the projected value showed the position of MSL riverbank line. Subsequently, Line of Sight (LOS) was used to setting up a baseline representing 1.043 m at LAT level and 2.302 m at MSL level. Both MSL and LAT values referred as the measured value of the initial cross-section line's and endpoint. If the initial point is below 1.043 m, we must reduce the value to 1.043 m. If the endpoint is higher than 2.302 m, we must reduce the value to 2.302 m. Then, we inserted the newly derived value to simulate the MSL baseline, representing the water level at 2.302 m MSL and 1.043 m LAT, as illustrated in Figure 4.

Every cross-section line went through the same process to identify MSL points, as shown in Figure 5. It generated the derived coordinate as the point feature in ArcGIS software. Then, the coordinates have been connected to form a yellow line across all points. The generated MSL riverbank line in Figure 5 is not smooth since we generated only a few points. The curved line required more connected points to produce a smooth riverbank line. However, that line still can consider as the true MSL riverbank line and a corrected riverbank line. Based on Figure 5, most of the yellow lines (MSL

riverbank line) were at the middle of low and high tide, and thus fulfilled the principle of tidal characteristic.

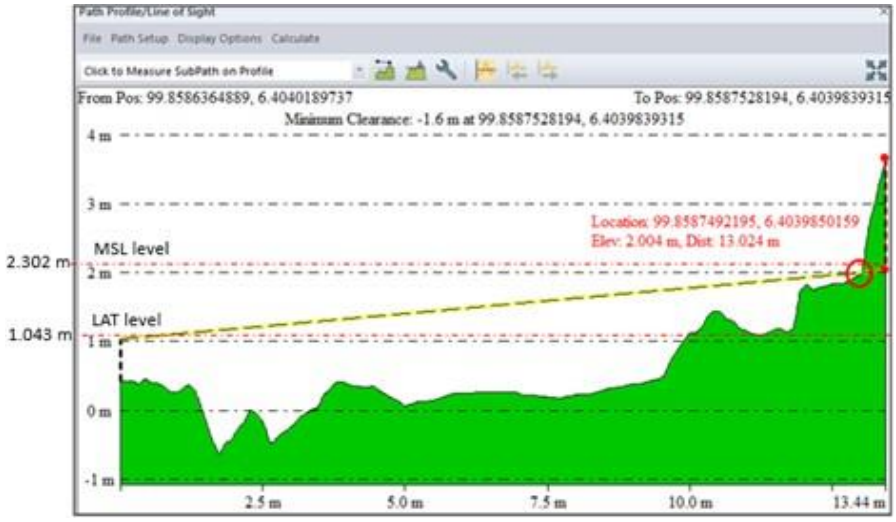

Figure 4. Slope analysis for UAV-MSL derived riverbank line.

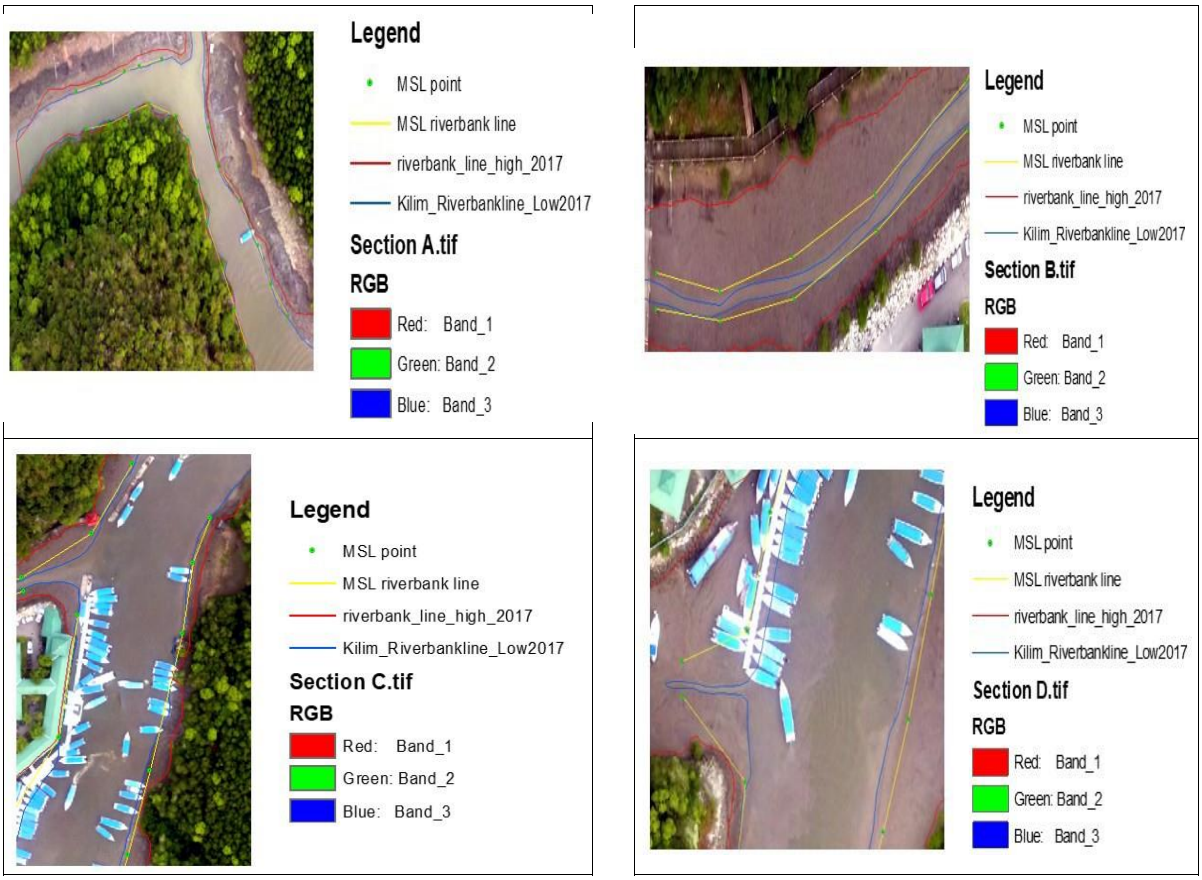

Figure 5. UAV-MSL derived riverbank line from UAV photogrammetry at Kilim River; Section A; Section B; Section C; Section D.

3.2. Accuracy Assessment of UAV-MSL and Tide Gauge Derived Riverbank Line

We compared the UAV-MSL derived riverbank lines to tide gauge-MSL data using the Root Mean Square Error (RMSE) analysis. RMSE determined the relationship of both datasets based on 30 coordinates of the point established at UAV-MSL and also points at tide gauge-MSL data. The total RMSE for northing between UAV-MSL and tide gauge-MSL derived riverbank line is 0.000048 m, and the total RMSE for easting is 0.00014 m. We generated the correlation model in Figure 6 to relate both MSL coordinates, and the R2 value is 0.9288, showing the substantial relationship value between both parameters.

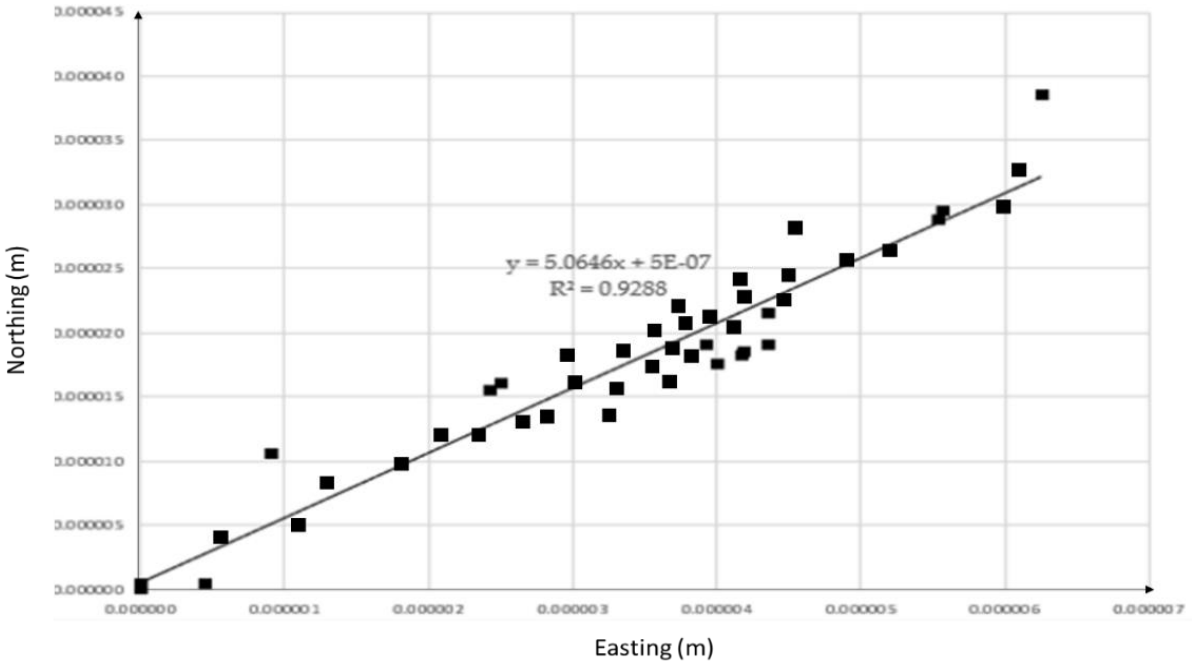

Figure 6. The correlation model of the relationship between UAV-MSL and tide gauge-MSL point.

4. Conclusion

In conclusion, the integration of geodetic, tidal, and UAV data is vital to derive the Kilim River's MSL riverbank line. The result in Figure 5 illustrates the UAV-MSL derived riverbank line position at Kilim River. We identified it at the intersection of MSL value (2.302 m) and chart datum (1.043 m). We considered this riverbank line as an exact riverbank line since it referred to the MSL value which calculated throughout December 2017. Integrating the aerial imagery from the UAV platform and tide gauge data could verify both data relationship and accuracy. Perhaps this study is beneficial for researchers in coastal geomorphology, hydrology, and geology to explore the earth's surface changes at the mangrove and coastal area by incorporating tidal data in their study for future work.

References

[1] Guariglia A, Buonamassa A, Losurdo A, Saladino R, Trivigno M L, Zaccagnino A, and Colangelo A 2006 *A multisource approach for coastline mapping and identification of shoreline changes. Annals of Geophy*. 49 1

[2] Lo K F A, and Gunasiri C W 2014 *Impact of coastal land use change on shoreline dynamics in Yunlin County, Taiwan Environ.* 1 2 124-136

[3] Garland G G 2010 *Rising sea level and long-term sustainability of near-shore islands of the United Arab Emirates: an approach to establishing setback lines for Abu Dhabi*. *Trans. Eco. Env*. 130 pp 135-146

[4] Zarillo G A, Kelley J, and Larson V A 2001 *GIS-Based Tool for Extracting Shoreline Positions*

from Aerial Imagery (Beach Tools). Engineer Research and Development Center Vicksburg Ms Coastal and Hydraulics Lab, 4 73

[5] Hamid A I A, Din A H M, Hwang C, Khalid N F, Tugi A and Omar K M 2018 *Contemporary sea level rise rates around Malaysia: Altimeter data optimization for assessing coastal impact. J. of Asian Earth Sc. 166, pp.247-259*

[6] Fricke A T, Nittrouer C A, Ogston A S, Nowacki D J, Asp N E and Souza P W F 2019 *Morphology and dynamics of the intertidal floodplain along the Amazon tidal river*. *Earth Surf. Process Landforms* 44 1 pp 204-218

[7] Mao X, Enot P, Barry D A, Li L, Binley A and Jeng D S 2006 *Tidal influence on behaviour of a coastal aquifer adjacent to a low-relief estuary*. *J of Hydrology* 327 pp 110-127

[8] Pugh D T 1996 *Tides, surges and mean sea-level: a handbook for engineers and scientists*. (New York: Wiley–Interscience)

[9] Mohamad N, Khanan M F A, Ahmad A, Din A H M, and Shahabi H 2019 *Evaluating water level changes at different tidal phases using UAV photogrammetry and GNSS vertical data*. *Sens.* 19 17 3778

[10] Mohamad N, Khanan M F A, Musliman I A, Kadir W H W, Ahmad A, Rahman M Z A, Jamal M H, Zabidi M, Suaib N M, and Zain R M 2017 *Riverbank erosion mapping using high resolution satellite image and unmanned aerial vehicle (UAV) approach*. Proc. 1st Int. Und. Post. Stud. Conf. Marine Sc. Tech. Management Kuala Terengganu pp 211-222

[11] Mohamad N 2019 *Evaluation of Riverbank Erosion Based on Mangrove Boundary Changes Identification Using Multi-Temporal Satellite Imagery*. Master Thesis, Universiti Teknologi Malaysia, Faculty of Built Environment & Surveying

Acknowledgments
The authors feel grateful to the Universiti Teknologi Malaysia for funding this manuscript under UTM High Impact Research (UTM HR) Vote Q.J130000.2452.09G29 and provide UTM Zamalah scholarship scheme. Great appreciation also to the people who sharing ideas and provide technical support throughout this study.